IN-LINE OPTICAL FIBER HOLOGRAPHY

by

WALID SALEH

Thesis submitted to the Faculty of the

Virginia Polytechnic Institute and State University

in partial fulfillment of the requirement for the degree of

Master of Science

in

Electrical Engineering

APPROVED:

Richard O. Claus

R. O. Claus, Chairman

G. I. Indebetouw

R. O. Pieper

June 1990

Blacksburg, Virginia

IN LINE OPTICAL FIBER HOLOGRAPHY

by

Walid Saleh

Committee Chairman: R. O. Claus

Electrical Engineering

(ABSTRACT)

The objective of this thesis is to demonstrate the feasibility of developing holograms in the cladding region of an optical fiber. The cladding is first stripped and replaced with dichromated gelatin (DCG) which is a highly efficient holographic storage medium. The evanescent field of the fiber is used as the reference beam to form an interference pattern with an object wave. The interference of the two fields is recorded in the DCG and forms the hologram. The holograms recorded have a grating type structure and can be utilized for guiding light selectively in and out of the fiber.

Acknowledgements

Many sincere thanks to Rick Claus for support, encouragement, and enthusiasm in helping me complete the series of experiments.

Thanks to both Guy Indebetouw, for many useful suggestions, and to Ron Pieper for taking time to be members of my committee.

The assistance from Russ May throughout the project was truly outstanding. Russ is an extremely superb mentor and a very good friend.

The help and assistance I received from all the members of FEORC cannot and will not be forgotten. Kent Murphy and Mike Gunther are two FEORC'ers that must be commended.

And last, but in no way least, special thanks to my lovely wife, Jamila, for believing in me, bearing with me and without whom much of this work would have been impossible.

CONTENTS

Figures and Tables

CHAPTER ONE

1.0 INTRODUCTION

The last fifteen years have been witness to a rapid increase in attention to using optical fibers in holography [1-56]. Optical fibers have been used to transmit holographic images for recording and reconstruction at locations remote from an actual test object [5, 49, 40]. Single mode fibers have been utilized as illuminators for holographic interferometry [23, 40, 19]. Fiber bundles and large diameter individual fibers have been used as flexible illuminators for pulsed laser holography [30, 38, 1, 39]. Individual fibers and coherent fiber bundles have also been used in local and remote holographic systems including double exposure [47, 20, 49, 40], time average [2], and real-time [29, 37, 4] systems. A holographic spatialy matched filter for in-line signal processing in optical fibers has also been developed at the Fiber and Electro-Optics Research Center at VA TECH [paper to be published]. The major thrust of all these efforts has, however, been to use the optical fiber as a convenient tool to guide light to or from an object or a hologram.

Efforts to produce interference gratings in or along optical fibers have also been on the increase in recent years [57-60]. Photosensitivity of a germanium-doped core has been exploited to form longitudinal Bragg reflection gratings for

use as a high resolution spectrometer [57]. A photoresist grating placed in the evanescent field region near the core of a side-polished fiber has been the key element of a proposed single mode optical fiber spectrometer [58]. A similar photoresistive technique has been used to fabricate surface-relief gratings for narrow band filtering in optical fibers [59]. Intense beams of ultraviolet light have been used to impress a phase grating along the core of an optical fiber [60].

The holograms this thesis deals with are recorded in a layer of holographic storage material coated in the cladding area of an optical fiber. The cladding has been ground down to an extent that the evanescent field of the fiber interacts with the holographic storage material. The evanescent field (u_r) is used as both the reference wave for recording and the read-out wave for the reconstruction of the hologram. To make the hologram, the evanescent field (u_r) is superimposed on an object wavefield (u_o) to form an interference pattern. The interference pattern is recorded in a very narrow region in the holographic storage material. The penetration depth of the evanescent wave thus determines the thickness of the hologram. The hologram also exhibits a "grating-type" structure due to the nature of the interference phenomena.

Similar waveguide holograms have been investigated in conventional planar optical waveguides [61-67] and a thorough

theoretical treatment has been given [62]. A fair amount of research has been performed along these lines [63-65]. Holograms of test objects have been made in a recording layer on a waveguide film using a plane reference wave to record the hologram [63]. Formation of holographic gratings by the interference of two guided modes has been investigated both experimentally [64] and theoretically [65].

All the papers involving holography and waveguides have been restricted to experimental or theoretical investigations of grating type holograms along conventional planar optical waveguides. To my knowledge there has been no attempt to implement the expertise gained by working with waveguides and holographic storage materials, such as dichromated gelatin (DCG), to optical fibers. As mentioned before, holography with optical fibers has been performed with lower efficiency holographic storage materials such as photoresist, but no experiments have been reported with dichromated gelatin (DCG), the highest efficency holographic storage material. It is the primary attempt of this thesis to demonstrate experimentally the feasibility of developing a grating hologram in dichromated gelatin along the cladding region of an optical fiber. Holograms of this type may turn out to be extremely useful for various applications both in the research environment and in industry.

CHAPTER TWO

2.0 PRINCIPLES OF EVANESCENT WAVE HOLOGRAPHY WITH OPTICAL FIBERS:

The electric field distribution within an optical fiber is periodic inside the core and evanescent outside of this region. The basic underlying idea of evanescent wave holography with optical fibers is to use an evanescent wave as the reference and/or read-out wave.

The distance to which the field extends outside the core is typically on the order of the wavelength of the light propagated and greatly depends on the order of the mode (higher order modes penetrating further). Due to the small penetration depths, the core region and the hologram storage material must be in direct optical contact. The refractive indices must also fulfill the condition for total internal reflection:

$$n_{core} > n_{storage}$$

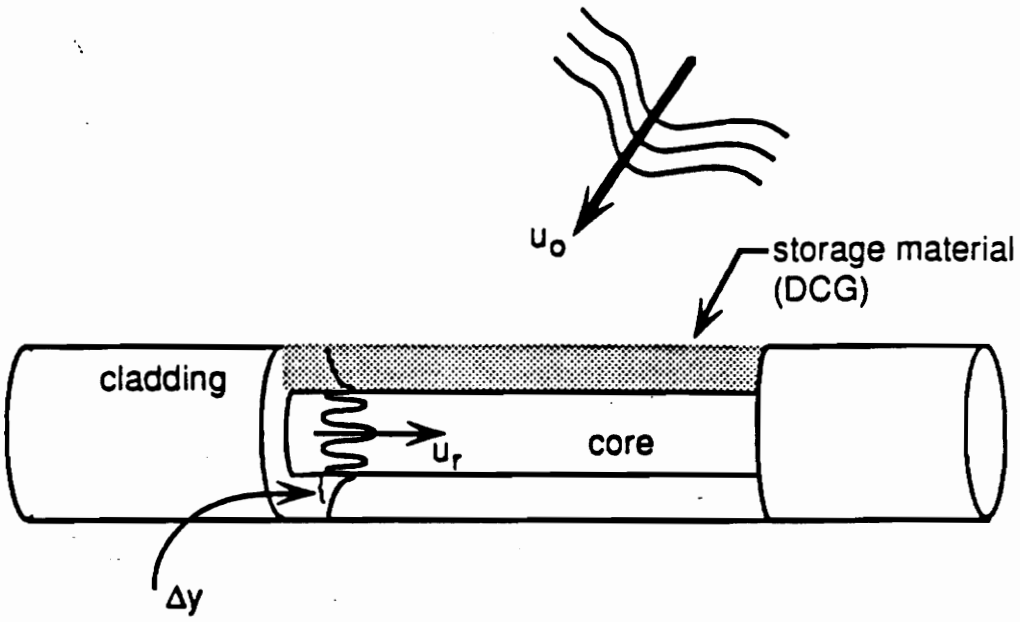

Figure 2.1

Figure 2.1 schematically shows the recording of the hologram in an optical fiber.

The electric field distribution of a guided mode is considered. Its evanescent part outside the core is the reference wave u_r. The object field u_o interferes with u_r and this interference is recorded in a storage material. The depth to which the actual hologram extends into the cladding is thus given by the penetration depth Δy of the evanescent wave and not by the cladding thickness or the storage material thickness (given that the storage material thickness is much larger than the penetration depth of the evanescent wave). The storage material must hence be able to sustain volume holograms and not surface relief holograms since the latter would require a storage material thickness which is small compared to the penetration depth of the evanescent wave. The theory developed in this paper describes volume holograms made with evanescent waves.

The refractive index of the storage material must have a high modulation ability since the effective thickness of the hologram is determined by the penetration depth of the evanescent wave. If a storage material with a weak modulation of the refraction index is used, we must compensate for this by making the recording layer thicker. This would be useless due to the limited penetration depth of the evanescent wave and thus high modulation of the refraction index is desired. It is for this fundamental reason that dichromated gelatin is chosen as the storage medium compared to other materials (such

as photoresist) which have been used before [58]. Highest reported diffraction efficiencies of photoresist is 60% where this number is 90% for dichromated gelatin [68].

Using a plane wave as the object wave will result in a hologram structure of regular periodic shape. The assumption is that the interference of u_o and u_r in the storage material will produce a proportional variation of the index of refraction which is periodic along the fiber, and exponentially decaying in a direction transverse to the fiber. Figure 2.2 shows this schematically.

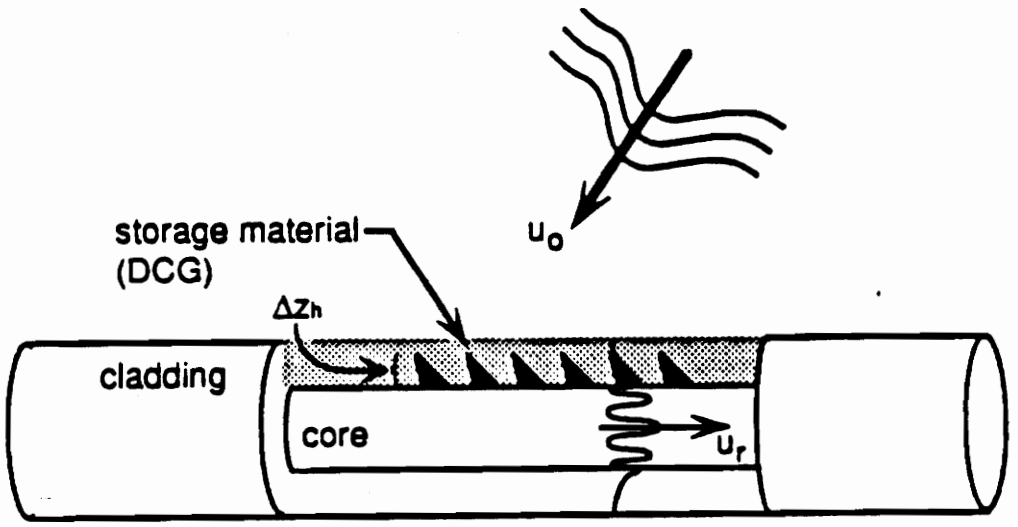

Figure 2.2

The slanted lines extending a distance $\blacktriangle Z_H$ into the storage material indicate loci of constant refractive index.

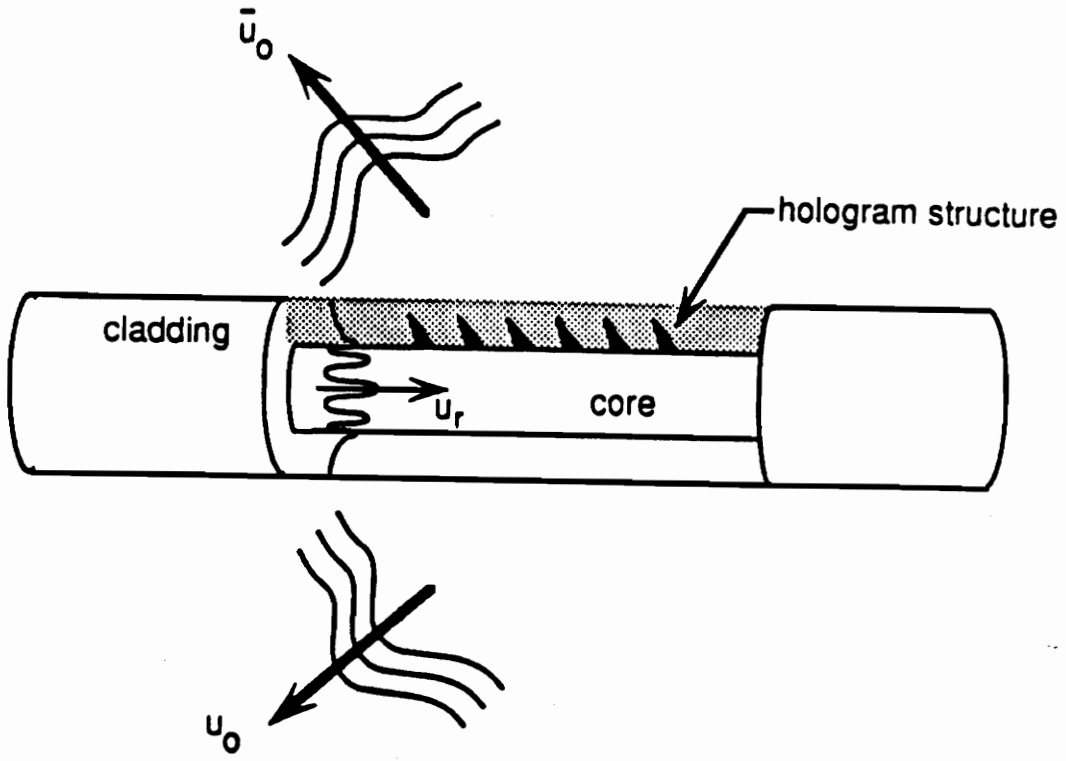

Figure 2.3

Figure 2.3 shows the reconstruction of the hologram.

The guided read-out wave u_r is propagating in the same direction as the reference wave did. This is diffracted by the hologram structure and reconstructs the object field u_o. In addition to u_o, a second weaker field $\bar{u}_o$ is generated which is a mirror image of u_o with respect to the $z = 0$ plane.

The condition for reconstructing the object wave exactly is that the read-out wave be identical to the reference wave. In other words the read-out and reference waves must have the same wavelengths and mode numbers for exact reconstruction of the object wave. The mirrored field $\bar{u}_o$ is generated by the diffraction of the read-out wave by the hologram and is not a reflection of any type from the boundaries. Reflection of the object field u_o does take place and only contributes minimaly to the intensity of $\bar{u}_o$.

In principle, reconstruction is also possible by any of the following methods shown here schematically in figures 2.4, 2.5, and 2.6.

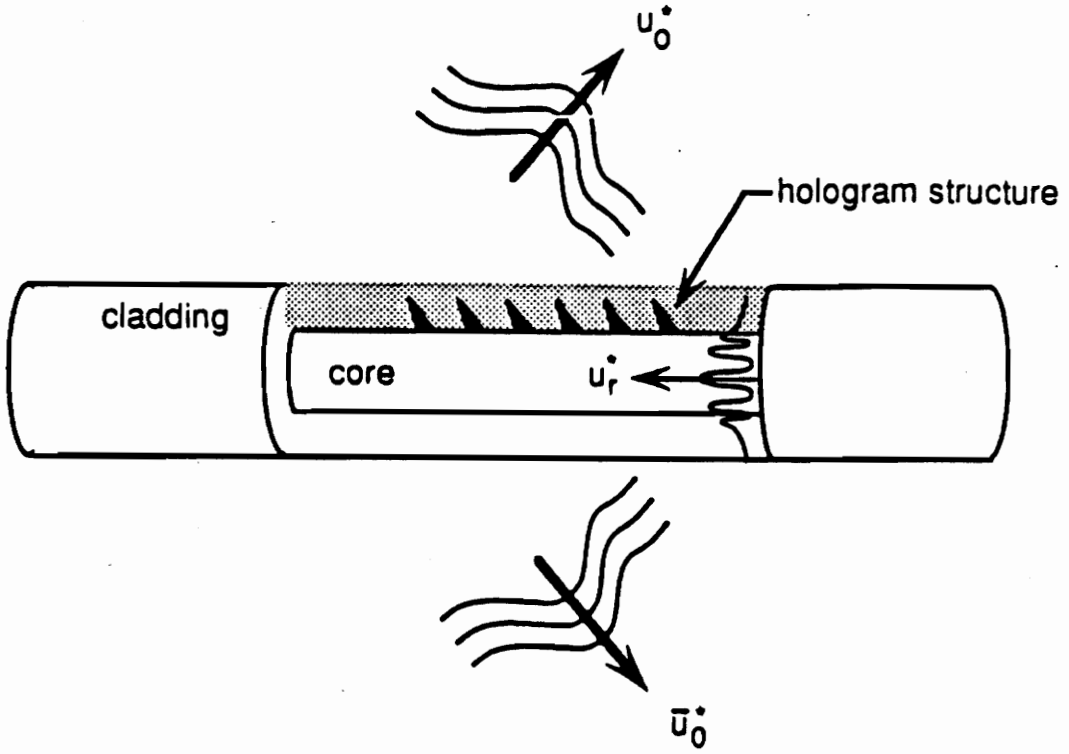

Figure 2.4

Illumination of the hologram with the conjugate reference wave u_r^* results in the conjugate object wave u_o^*. u_r^* has the same mode number as u_r except that it is travelling in the opposite direction.

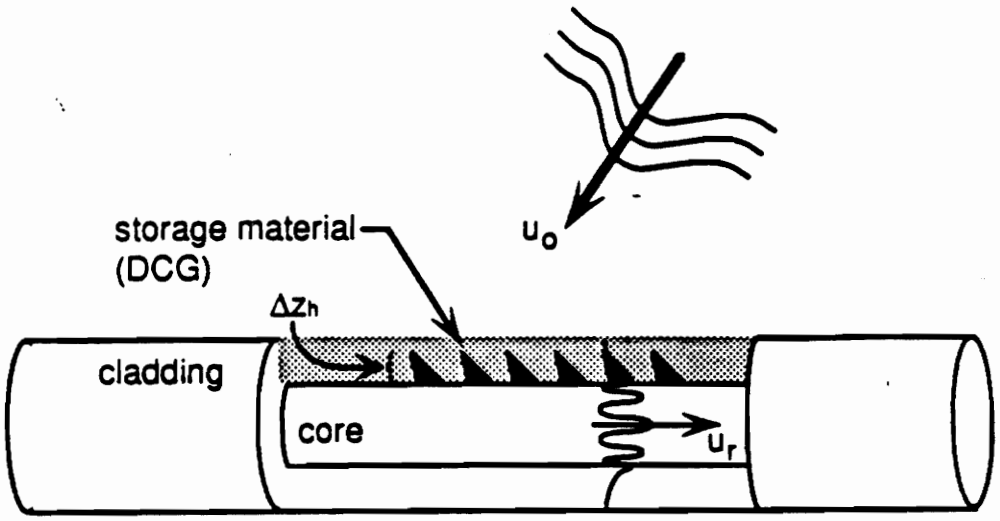

Figure 2.5

Illumination of the hologram with the object wavefield u_o results in the guided wave u_r. This case is of importance especially if the object wavefield is a laser beam (which approximates a laterally limited plane wave) in which case we have a type of a grating coupler.

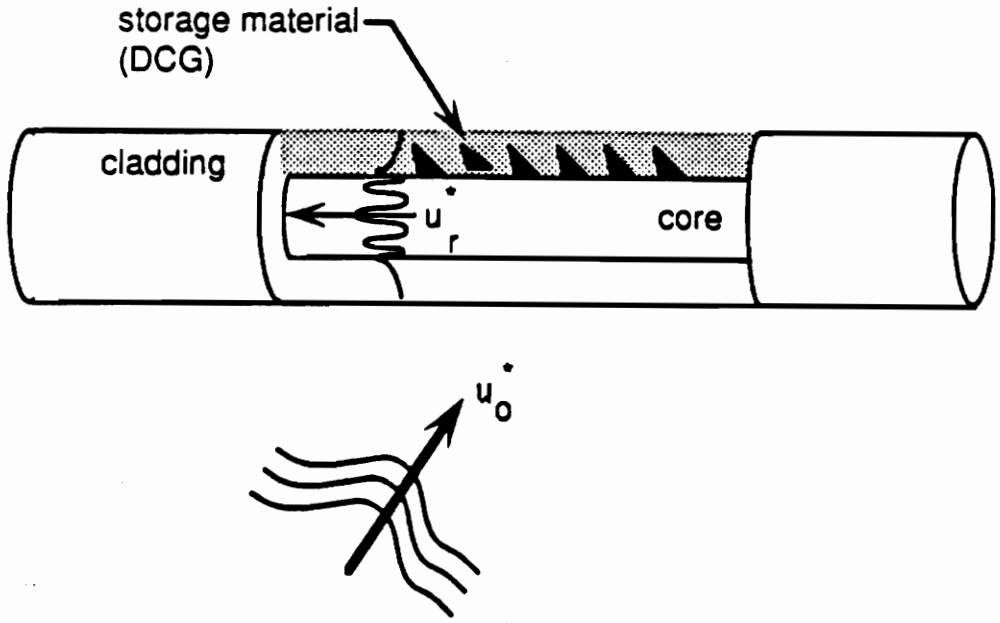

Figure 2.6

Illumination of the hologram with the conjugate object wavefield u_o^* resulting in the conjugate reference wave u_r^* . Again we have a type of grating coupler as in the previous figure.

CHAPTER THREE

3.0 THEORY

The theory presented in this chapter describes holograms with a plane wave as the object wave and the evanescent part of a guided wave inside the optical fiber as the reference wave. The theory is adapted from reference 62 and is presented here with the particular case of evanescent wave holography with optical fibers in mind. The recording of the hologram is discussed first in section 3.1 and the reconstruction process is presented in section 3.2. A brief discussion on diffraction efficiencies is also given in section 3.3.

The following table is presented to facilitate reading and to clarify symbols and notations used.

TABLE 3.1

u_e	evanescent wave
u_p	plane wave
n	refractive index of recording medium
n'	refractive index of surrounding medium
	mean refractive index of surrounding medium
z_o	thickness of recording medium
u_c'	illuminating wave
u_d'	diffracted wave

Note that waves with a "prime" are outside the recording medium and "unprimed" waves are inside the medium.

Also note that the subscripts 'd' denotes diffracted, 'c' denotes illuminating or reconstructing, 'e' denotes evanescent, and 'p' denotes plane.

3.1 RECORDING OF THE HOLOGRAM:

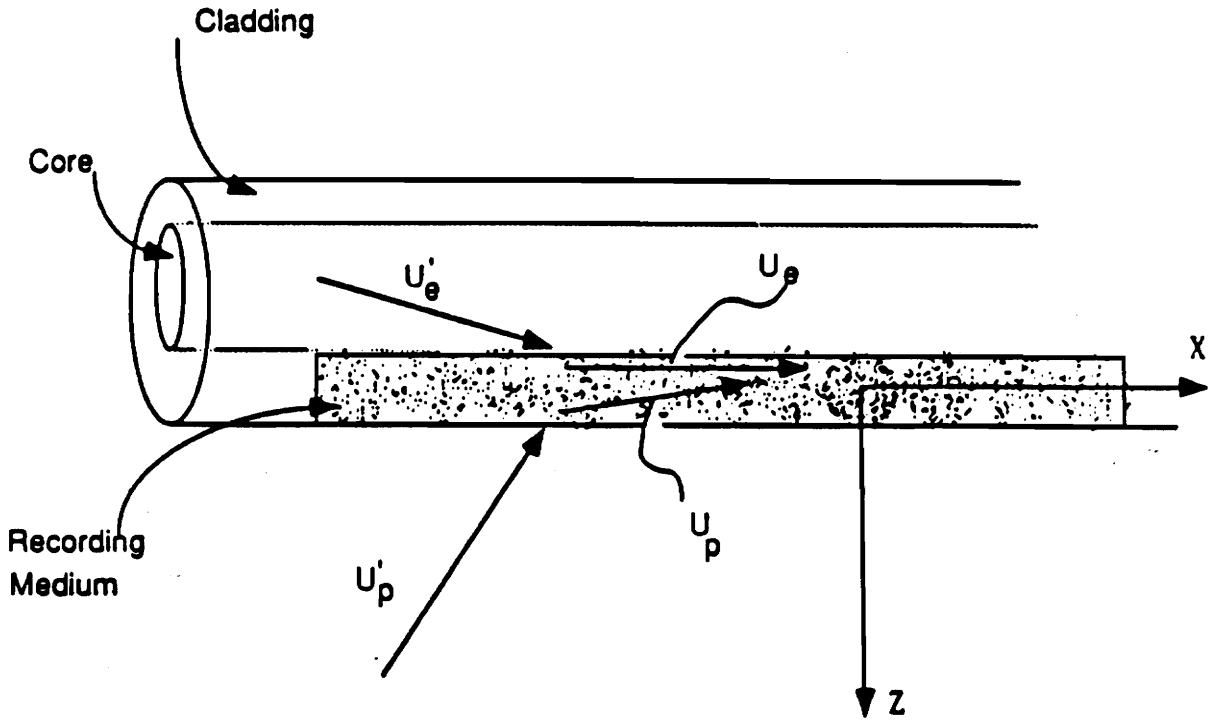

Figure 3.1

The recording of the hologram is schematically shown in Figure 3.1.

u_e' is the ray that exceeds the critical angle within the core region and creates the evanescent wave u_e inside the recording medium. u_p' is the plane wave incident upon the recording medium and u_p is the transmitted part within the recording medium, which interferes with u_e.

Assuming TE-polarized vectors we have:

$$E_y(x,z) = u(x,z) \qquad (3.1)$$

$$E_x = E_z = 0;\ H_y = 0$$

$$H_x(x,z) = (-1/jwu_o)(\delta u/\delta z);$$

$$H_z(x,z) = (-1/jwu_o)(\delta u/\delta z)$$

The time dependence exp(-jwt) is omitted and all fields are assumed periodic with angular frequency w.

In the recording medium we have:

$$u_e(x,z) = u_e \exp[j(k_{ex}x + k_{ez}z)] \qquad (3.2)$$

$$= u_e \exp[jk_{ex}x] \exp[-|k_{ez}|z], \quad \text{ie } k_{ez} = j|k_{ez}|$$

where

$$k_{ex} > k, \quad \text{and } k_{ez} = j[(k_{ex})^2 - k^2]^{1/2}. \qquad (3.3)$$

Also,

$$u_p(x,z) = u_p \exp[j(k_{px}x + k_{pz}z)]. \qquad (3.4)$$

with

$$k_{pz} = [k^2 - (k_{px})^2]^{1/2}. \qquad (3.5)$$

The amplitudes of u_e and u_p in the recording medium can be obtained from $u_{e'}$ and $u_{p'}$, respectively, with the Fresnel transmission coefficients:

$$u'/u = t_s = 2k_z/(k_z + k_z'); \quad r_s = t_s - 1. \qquad (3.6)$$

The intensity is defined as:

$$I(x,z) = \langle E^2(x,t) \rangle = (1/2).\ u^*(x,z)u(x,z). \qquad (3.7)$$

Assuming k_{ex} = real ie. no absorption in recording medium then the intensity of the interference of u_e and u_p is:

$$\begin{aligned} I(x,z) &= 1/2[u_p(x,z) + u_e(x,z)]^* [u_p(x,z) + u_e(x,z)] \qquad (3.8) \\ &= 1/2\{ |u_p|^2 \exp[j(k_{pz} - k^*_{pz})z] + |u_e|^2 \exp(-2 |k_{ez}|z) \\ &\quad + u_e^* u_p \exp[j[(k_{px} - k_{ex})x + (k_{pz} - k^*_{ez})z]] \\ &\quad + u_e u^*_p \exp[j[(k_{ex} - k_{px})x + (k_{ez} - k^*_{pz})z]]\}. \end{aligned}$$

For our case where u_p is a plane wave, (i.e. k_{pz} is real), this expression reduces to

$$\begin{aligned} I(x,z) &= 1/2(|u_p|^2 + |u_e|^2 \exp(-2|k_{ez}|z) \qquad (3.8a) \\ &\quad + 2\mathrm{Re}(u^*_e u_p \exp(j[(k_{px} - k_{ex})x + k_{pz}z])) \exp[-|k_{ez}|\ z]. \end{aligned}$$

Inspection of equation 3.8 shows that an identical intensity distribution would result if the waves $u^*_e(x,z)$ and

$u^*_p(x,z)$ interfere instead of $u_e(x,z)$ and $u_p(x,z)$. Complex conjugation is of course equivalent to the time-reversal transformation t to -t. The waves u_e^* and u_p^* can then be understood as u_e and u_p, respectively, traveling in the opposite direction.

The theory presented until now is fairly straightforward and no consequential assumption is made. Now the assumption is made that the photosensitive or recording medium is homogeneous and weakly absorbing and equation 3.8 is a fairly good approximation to the intensity distribution I(x) in the medium. Furthermore, the response of the recording medium to this intensity distribution is that the dielectric constant, ϵ, is a linear function of the local intensity. In other words

$$\epsilon(x) = f[I(x)\tau]$$

where τ is the exposure time. The recorded hologram is therefore a dielectric grating with

$$\epsilon(x,z) = \bar{\epsilon} + \bar{\delta}\epsilon(x,z) \qquad (3.9)$$

where

$\bar{\epsilon}$ = mean dielectric constant of hologram,

and

$\bar{\delta}\epsilon(x,z)$ = spatial variation of ϵ due to the interference

$$= 1/2\ A\ d\epsilon/dI(u^*_e\ u_p\ \exp(j[(k_{px} - k_{ex})x$$

$$+ (k_{pz} - k^*_{ez})z]) + u_e\, u_p^*(j[(k_{ex} - k_{px})x$$

$$+ (k_{ez} - k^*_{pz})z])\}. \qquad (3.10)$$

Written in the form of 3.8a, this becomes

$$\bar{\delta}\,\epsilon(x,z) = A\, d\epsilon/dI\ \mathbf{Re}\{u^*_e\, u_p \exp(j[(k_{px} - k_{ex})x + (k_{pz})z\}$$

$$\exp(-|k_{ez}|z) \qquad (3.10a)$$

Non-linearities of $f[I(x)\tau]$ are neglected and variations of ϵ due to intensity variation of u_e are assumed constant (ie. $d\epsilon/dz$ constant). The constant 'A' is the average of $\bar{\delta}\,\epsilon(x,z)$ integrated along the z-axis.

Since a linear function f was assumed, $\bar{\delta}\,\epsilon(x,z)$ can be thought of as having two separate interference terms. These are

$$\bar{\delta}\,\epsilon(x,z) = \delta\epsilon_1(x,z) + \delta\epsilon_2(x,z), \qquad (3.11)$$

where

$$\delta\epsilon_1(x,z) = 1/2\ A\ (d\epsilon/dI)\ u_e^*\, u_p \exp(j[(k_{px} - k_{ex})x +$$

$$(k_{pz} - k^*_{ez})z]). \qquad (3.12)$$

and

$$\delta\epsilon_2(x,z) = 1/2\ A\ (d\epsilon/dI)\ u_e\, u^*_p \exp(j[(k_{ex} - k_{px})x$$

$$+ (k_{ez} - k^*_{pz})z]) \qquad (3.13)$$

The significance of this shall become clear later.

It should be noted that the interference fringes are periodic in the x-direction and multiplied by an exponential

decay in the z-direction. The fringes are slanted with an angle α where:

$$\tan \alpha = k_{pz}/(k_{ex} - k_{px}) \qquad (3.14)$$

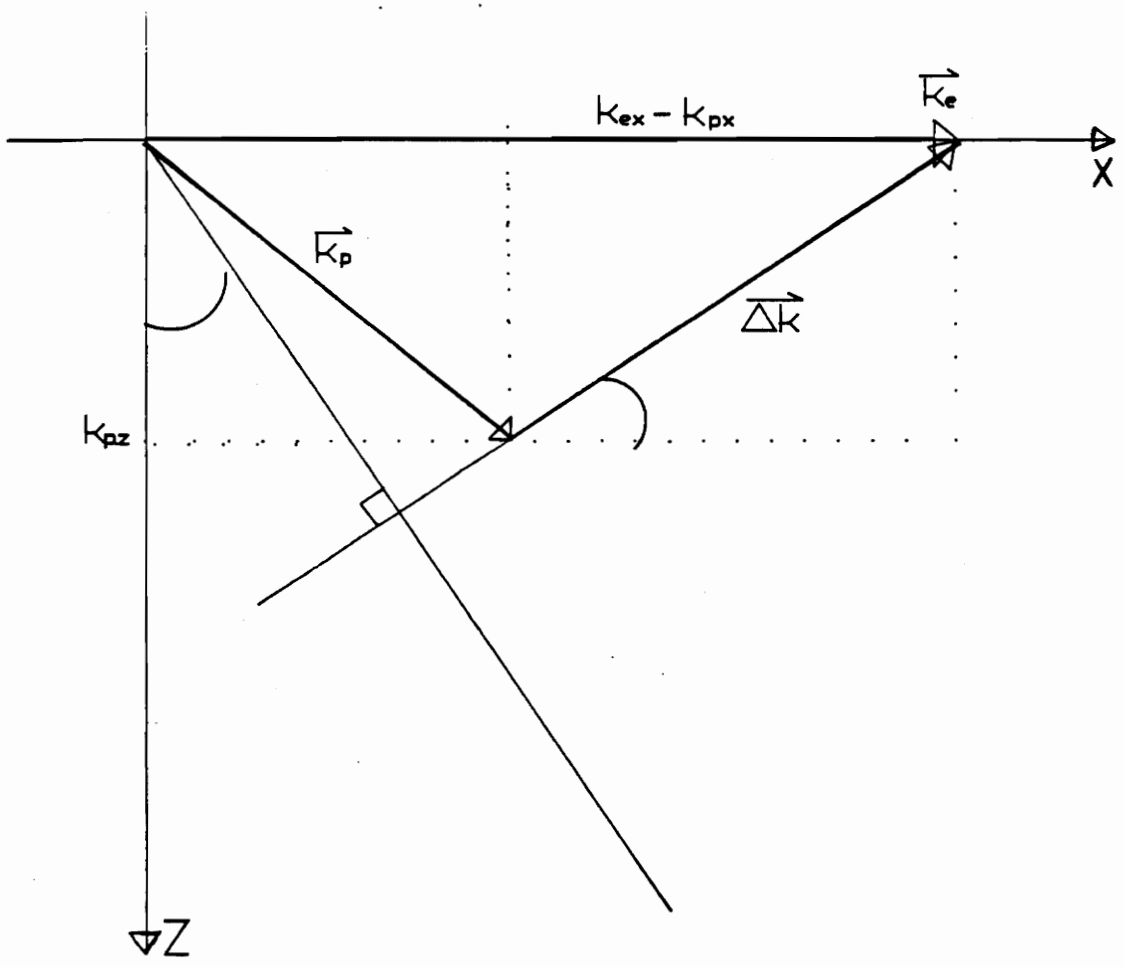

Figure 3.2

Figure 3.2 is a vector diagram which shows the various angles and vectors involved

3.2 RECONSTRUCTION OF THE HOLOGRAM

Reconstruction of the hologram can, in principle, be accomplished in different configurations as explained in Chapter 2. Here it is assumed that the hologram is illuminated with a TE-polarized plane wave u_c' where the frequency may be different from the frequency used to record the hologram. Here,

$$u'_c(x,z) = u'_c \exp[j(k'_{cx}x + k'_{cz}z)] \qquad (3.15)$$

where

$$k'_{cx} = \bar{k}'\sin\theta_c \quad \text{and} \quad \bar{k}' = \bar{n}'w_c/c \qquad (3.16)$$

with

θ_c = incident angle, and

$\bar{n}'$ = mean refractive index of surrounding medium.

The time dependence $\exp(-jw_ct)$ is again omitted.

The total field inside the hologram can be represented as

$$u(x,z) = u_c(x,z) + u_d(x,z) \qquad (3.17)$$

where

$u_c(x,z)$ = illuminating wave

$u_d(x,z)$ = diffracted wave

$u(x,z)$ must satisfy the wave equation

$$[\delta^2/\delta^2x + \delta^2/\delta^2z + (w_c/c)^2\,\epsilon(x,z)]\,u(x,z) = 0 \qquad (3.18)$$

This is solved by successive approximation (see ref.61) and we find $u_c(x,z) = u_c \exp[j(k_{cx}x + k_{cz}z)]$ (3.19)

where $k'_{cx} = k_{cx}$

and
$$k_{cz} = \begin{cases} -[k^2 - (k_{cx})^2]^{1/2} & \text{if } |k_{cx}| \leq \bar{k} \quad (3.20a) \\ j[(k_{cx})^2 - k^{-2}]^{1/2} & \text{if } |k_{cx}| > \bar{k} \quad (3.20b) \end{cases}$$

Equation 3.20a describes the reconstruction of the form indicated in Figures 2.3 and 2.4. Equation 3.20b describes the reconstruction of the form indicated in Figures 2.5 and 2.6.

Solving for u'_d, the assumption is made that the penetration depth of the evanescent wave is much larger than the thickness of the recording medium, z_o. The wavelets scattered by each volume element of the hologram are calculated using a Green's function and integrated over the volume of the hologram (see ref. 61).

u_d is found to have two components:

$$u_d(x,z) = u_d(x,z = 0) + u_d(x,z = z_o) \quad (3.21)$$

where

$$u_d(x,z = 0) = (w_c/2c)(d\epsilon/dI)u_c\, u^*_e\, u_p \exp(jk_x x)/ k_z(k_z + k_{cz} + k_{pz} - k^*_{ez}) \quad (3.22)$$

$$u_d(x,z = z_o) = (w_c/2c)(d\epsilon/dI)u_c\, u_e^*\, u_p \exp[j(k_x x + k_z z_o)]/ k_z(-k_z + k_{cz} + k_{pz} - k^*_{pz}) \quad (3.23)$$

where $k_{dx} = k_x = k_{cx} + k_{px} - k_{ex}$ (3.24)

$$k_{dz} = k_z = \begin{cases} (\bar{k}^2 - k_x^2)^{1/2} & \text{if} \quad |k_x| \le \bar{k} \\ j(k_x^2 - \bar{k}^2)^{1/2} & \text{if} \quad |k_x| > \bar{k} \end{cases} \tag{3.24a}$$

The physical interpretation of this result is that upon reconstruction of the hologram, two diffracted waves are generated. One is radiated toward the boundary $z = z_o$ and the other is radiated toward the boundary $z = 0$. These are denoted u^+_d and u^-_d, respectively and $k^+_{dx} = k_{dx} = k_x$.

Also,

$$k^+_{dz} = k^-_{dz} = \begin{cases} [k^2 - (k_{dx})^2]^{1/2} & \text{if } |k_{dx}| \le \bar{k} \\ j[(k_{dx})^2 - k^2]^{1/2} & \text{if } |k_{dx}| > \bar{k} \end{cases} \tag{3.25}$$

For our present case with optical fibers we are interested in only the observable parts which are transmitted into the surrounding medium. These observable parts are (a) when $|k_{dx}| \le \bar{k}$ and (b) when $\bar{k} < |k_{dx}| \le \bar{k}'$, with $\bar{k}' = \bar{n}' w_c/c$. The first case is obvious from the mathematics and both $u^+_d{}'$ and $u^-_d{}'$ (primed i.e. outside the recording medium; also the subscript 'd' denotes 'diffracted') are transmitted. The second case needs to be explained in more detail. When $\bar{k} < |k_{dx}| \le \bar{k}'$ we are left with evanescent waves at the boundary $z = 0$. $u^-_d{}'$ is thus radiated into the cladding with an

angle $\alpha'_d > |\alpha_{critical}|$ via the evanescent wave, but u^+_d (un-primed i.e. inside the recording medium) decays before it reaches the interface $z = z_o$ and is therefore not observable because it is confined within the core.

The figures presented in Chapter 2 can now be understood more clearly keeping in mind the dielectric structure (3.12 and 3.13). In Figure 2.3, illumination with the reference wave $u_r(x)$ reconstructs the object wavefield $u_o(x)$ by interaction with the term $u^*_r u_o$ in the dielectric structure of the hologram. Figure 2.4 is the case when the hologram is illuminated with the conjugate reference wave, u^*_r , and this interacts with the terms $u_r u^*_o$ in the dielectric structure of the hologram. In Figure 2.5, illumination is via the object wavefield, u_o, which interacts with $u_r u^*_o$ term of the hologram. Finally, Figure 2.6 is the case of illumination with the conjugate object wavefield, u^*_r, which interacts with the terms $u^*_r u_o$.

3.3 DIFFRACTION EFFICIENCIES

The diffraction efficiency , η , is defined as the ratio of the diffracted power, P_d, and the power of the illuminating wave P_c, both measured in the medium surrounding the hologram.

$$\eta = P_d/P_c \qquad (3.26)$$

Each of these powers is defined as the product of the illuminated area of the hologram, A, times the z component of the time averaged energy flow density, $\langle S_z \rangle$.

$$P = A \cdot \langle S_z \rangle$$

where $S = E \times H$ (all quantities are vectors)

and $$\langle S_z \rangle = [1/(2wu_o)]\ |u|^2\ \mathrm{Re}\{k_z\}$$

However, η is dependent on which terms in the dielectric structure (see 3.10 - 3.13) are being interacted with and two separate efficiencies are found. For interaction with $u^*_e u_p$ we have

$$\eta_+ \ (u^*_e u_p) = \eta_- \ (u^*_e u_p) = (w_c/c)^4 (d\epsilon/dI)^2\ |u_e|^2\ |u_p|^2 \cdot \frac{|k'_{cz}|}{|k'_{cz} + k_{cz}|^2} \cdot \frac{|k'_{dz}|}{|k'_{dz} + k_{dz}|^2} \cdot \frac{1}{|-k_{dz} + k_{cz} + k_{pz} - k^*_{ez}|^2} \qquad (3.27)$$

This is for the case $k_{dx} \leq \bar{k}$ and for the configurations of Figures 2.3 and 2.4. Note that if $\bar{k} \leq |k_{dx}| < \bar{k}'$, then

$$\eta_+ (u^*_e u_p) = 0 \qquad (3.28)$$

and

$\eta_-(u_e^* u_p)$ is given by equation 3.27

For the interaction with the term $u_e u^*_p$, we have for $|k_{dx}| < \bar{k}$: (3.29)

$$\eta_+ (u_e u^*_p) = \eta_-(u_e u^*_p) = (w_c/c)^4 (d\epsilon/dI)^2 |u_e|^2 |u_p|^2 \cdot$$

$$\frac{|k'_{cz}|}{|k'_{cz} + k_{cz}|^2} \cdot \frac{|k'_{dz}|}{|k'_{dz} + k_{dz}|^2} \cdot \frac{1}{|-k_{dz} + k_{cz} + k_{ez} - k^*_{pz}|^2}$$

for $\bar{k} \leq |k_{dx}| < \bar{k}'$, we have

$$\eta_+ (u_e u_p^*) = 0 \qquad (3.30)$$

and for $|k_{dx}| > \bar{k}'$, we have

$$\eta_+ (u_e u_p^*) = \eta_-(u_e u_p^*) = 0 \qquad (3.31)$$

CHAPTER FOUR

4.0 EXPERIMENT

The experimental part of this thesis consists of the most delicate and complex portion of the work performed. In this chapter, the attempt is to present the actual experiment performed and to pay as much attention to detail as necessary in order to clarify what is being discussed. This chapter consists of the following sections:

4.1) Fiber Preparation

4.2) Fiber Coating

4.3) Experimental Set-up

4.4) Sensitization of Gelatin

4.5) Exposure and Development

4.6) Data

4.1 FIBER PREPARATION:

The fiber utilized for the experiment is a Corning 1521 dual acrylate fiber. The core diameter is 9 um and the cladding diameter is 125 um. The fiber also has a cutoff wavelength of approximately 1200 nm. The decision to use these parameters is based upon the availablity of fiber and the fairly large cutoff wavelength which made it suitable for use with a blue-green laser.

A length of approximately 1.5 m of fiber is selected and the jacket is blade-stripped near the middle. The length that is stripped is approximately 6 cm. The buffer layer between the jacket and the cladding must be removed also as this will cause problems later. The fiber is now ready to be attached to special microscope-type slides prepared specifically for side-polishing of fibers.

The microscope-type slides are ordinary slides of glass of a 6 to 7 cm length and approximately 2 cm width. One side of the slide is rounded with a radius of curvature of 10 inches (see Figure 4.1.1). It is on this curved side that the fiber is attached for side-polishing.

The slides are placed in a wedge cut into a small block of wood so that they may stand upright with the curved portion on top. A thin layer of epoxy is spread onto the curved portion of the slide. The epoxy used is Revlon Clear Nail Polish which is chosen for its ease of spreading, relatively quick drying, and hardness. Before the epoxy dries, the stripped portion of the fiber is carefully placed on top and held slightly taut along the curved portion of the slide. It must be ensured that a small length (~ 0.5 cm) of un-stripped or jacketed fiber extends onto the slide at both ends as this will provide extra mechanical strength. Also, care must be taken so that the fiber is not placed near the edges of the slide but is near the middle of the thickness of the slide.

After the epoxy is relatively dry and the fiber is securely in place, an extra drop of epoxy is placed near the ends of the slide where the 0.5 cm of jacket is extending onto the slide. This is for extra mechanical strength (see Figure 4.1.1).

The fiber/slide combination is then allowed to dry overnight in such a position so that the fiber is free to hang vertically from the edges of the slide. Figure 4.1.1 is helpful in visualizing the above steps.

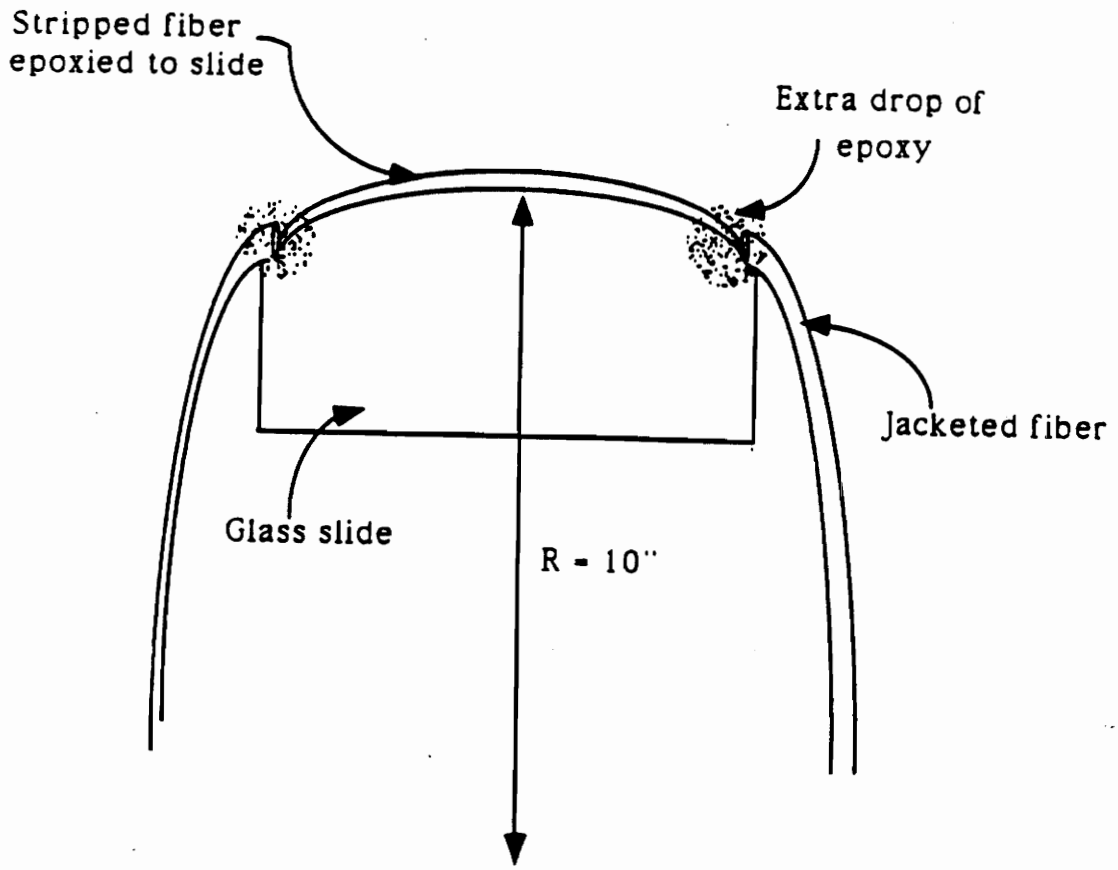

Figure 4.1.1

After the fiber/slide is allowed to dry overnight, the fiber is ready for side-polishing. The slide is attached to a special apparatus designed at FEORC for side polishing of fibers (Figure 4.1.2). A He-Ne laser beam is injected into the fiber and the output is constantly monitored via a power meter.

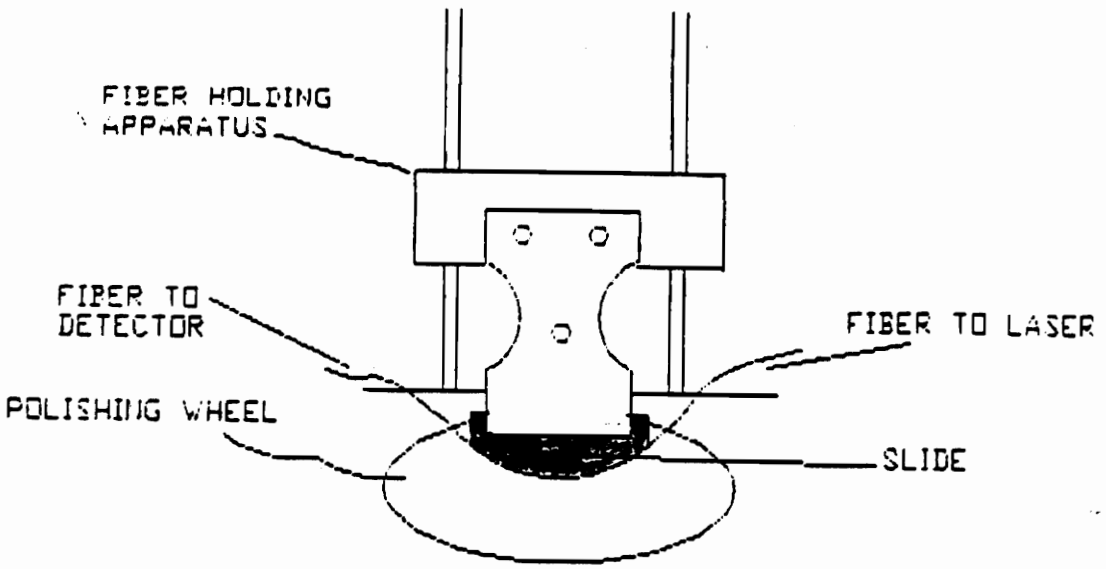

Figure 4.1.2

The slide is carefully lowered onto a polishing wheel which has a 0.3 um Aluminum oxide polishing pad. The wheel is turned on at a moderate speed while water is flowing on the polishing pad. The slide is gently moved radially inwards and outwards along the wheel. Care must be taken to move the slide radially and also to avoid the very center and the outer edge of the wheel otherwise mechanical stress is placed in the fiber and it is easily broken.

As the polishing is being performed the power going through the fiber is constantly being monitored. Since the fiber is in few mode operation, approximately 10% to 50% of its power is in the cladding region. As the side of the fiber is slowly polished and more of the cladding is removed, a portion of the cladding power escapes outside of the fiber. Generally, after 3 to 4 minutes of polishing an approximately 2 to 3 dB of power (approximately 30% to 40%) drop is encountered. This signifies that the evanescent region has been reached. At this point the slide is carefully removed and a drop of index matching fluid is placed on the polished portion of the fiber. The index matching fluid allows light to escape and eases the monitoring of the length of the portion of the cladding which has been removed. This length gives information as to how deep into the cladding we have penetrated as shown in Figure 4.1.3.

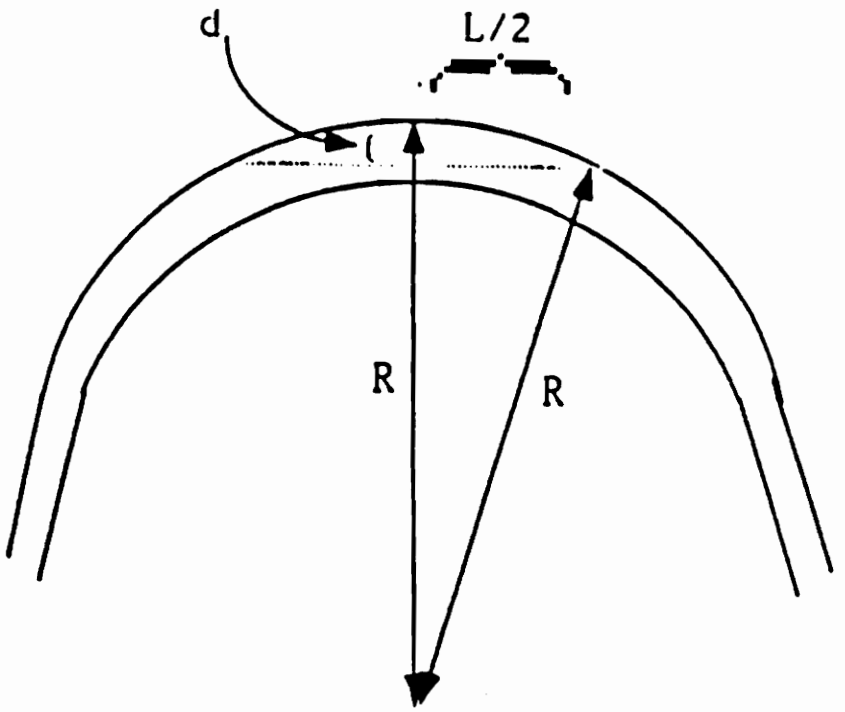

Figure 4.1.3

$R^2 = (L/2)^2 + (R - d)^2$

$[R^2 - (L/2)^2]^{1/2} = R - d$

$d = R - [R^2 - (L/2)^2]^{1/2}$ = depth penetrated into cladding

If the depth polished is found to be unsatisfactory, the fiber is once again placed onto the polishing wheel. In the experiments performed, the depth polished was generally between 40 and 55 um (The upper cladding layer is only ~ 60 um).

After the fiber has been polished to a satisfactory level, it is then ready for coating with gelatin.

4.2 FIBER COATING

Preparation of dichromated gelatin (DCG) film has been extensively discussed in the literature. Numerous methods and techniques for recording holograms in DCG films have been proposed. The number of variables affecting the outcome is enormous and strict control over every step of the process is necessary. For this reason, a detailed explanation of the steps and considerations involved in coating fibers for evanescent wave holography with DCG shall be presented here.

In preparing the DCG for coating of fibers in this experiment the general steps outlined in reference 61 were followed. The reason for this decision was that the experiments reported by reference 61 dealt with producing holograms along conventional planar optical waveguides utilizing the same principles of evanescent waves as discussed in the previous chapters.

The first obstacle that needed to be overcome was that discussed in chapter two and that is satisfying the condition for internal reflection

$$n_{core} > n_{DCG}$$

The reasoning followed for overcoming this obstacle is as follows. The index of refraction of the core is 1.458 and that of the cladding is 1.455. The index of refraction of water is approximately 1.3, therefore preparing a gelatin solution in water with the least amount of gelatin possible would raise the index of refraction of water by a very small amount. A 12%, by weight, solution of gelatin in water has an index of refraction of 1.54 (which further increases when sensitized, see section 4.4) [61] so the amount of gelatin needed for our experiments had to be less than 12%.

Another important consideration in determining an acceptable gelatin to water ratio was that if there was not enough gelatin present, the solution would be useless since it would not be able to sustain a useful hologram. This was tested by making ordinary microscope slide DCG plates and developing simple holograms as discussed later.

In tackling the above mentioned problems the following steps were performed. Starting with deionized water at 40°C, a certain weight of gelatin was gradually added and the

solution was stirred for approximately one hour. The gelatin to water ratio (by weight) was varied from 12% to 1% in increments of 1%. The gelatin used is Fisher gelatin with a bloom strength of 200.

Each time a solution was made, it was coated onto the fiber/slide by dipping the fiber/slide into it. The fiber/slide was then pulled out so that the polished edge of the fiber came out last and a fine film of gelatin clung to this polished edge. The thickness of the fine film remaining is not important as long as it is much larger than a few wavelengths of the light used for exposure (i.e. 441.6 nm). Care must be taken so that no air bubbles are allowed to cling to the fiber as this will distort the results. At this point the fiber is hung up for overnight drying in such a manner that the polished edge is facing down so that most of the gelatin is allowed to flow to the polished edge. The polished edge should be parallel to the ground so that a uniform film is coating the polished edge of the fiber.

When the gelatin has dried overnight, it is then prehardened for 15 minutes in Kodak Rapid Fix and rinsed in running water of approximately 22°C for another 15 minutes. The reason for the prehardening step is to make the gelatin insoluble in water when further processed. The film is again allowed to dry overnight in the same manner as discussed previously.

The film is now ready to be tested for the internal reflection condition. The test performed is as follows. Each time a film is prepared with a different gelatin content (varying from 12% to 1%), a He-Cd laser is injected into one end of the fiber. The idea is that if the condition for internal reflection is met, no light should escape from the polished edge of the fiber. This condition was met for gelatin solutions of 1%, 2% and 3%. However, when these concentrations were used to prepare conventional DCG plates (using ordinary microscope slides) and ordinary holograms of simple objects, all attempts failed. Since all other conditions were held constant, this indicated that these concentrations (1%, 2%, and 3%) were insufficient for sustaining useful holograms. A compromise had to be made between the amount of index mismatch tolerable between the fiber and DCG, and the ability to obtain useful holograms. For this reason the concentration of gelatin was again increased in increments of 1% until a satisfactorily conventional DCG plate and an ordinary hologram was obtained. Satisfactory results (ie. holograms using ordinary microscope slides) were achieved with gelatin concentrations of 5% and 6%. At 5% and 6% concentrations a small amount of light did escape near the polished edge of the fiber but this had to be tolerated in order to obtain useful holograms. All the

experiments reported from here on were performed with a gelatin concentration of 5%.

4.3 EXPERIMENTAL SET-UP

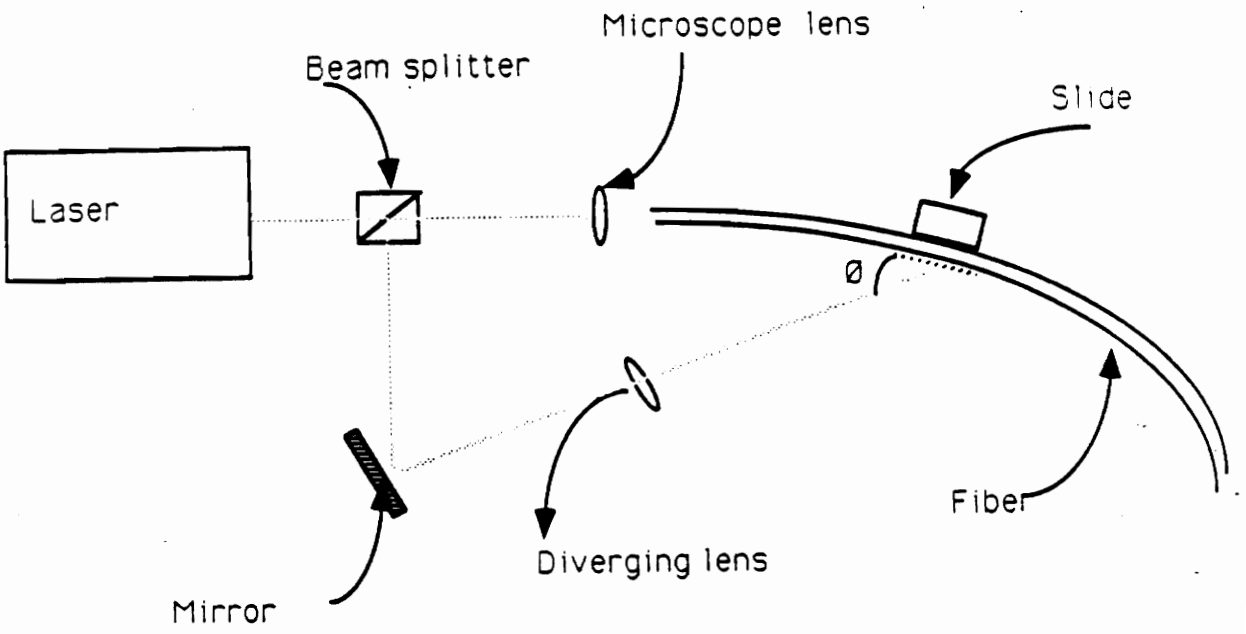

Figure 4.3.1

Figure 4.3.1 shows the experimental set-up.

A number of factors were kept in consideration upon arranging the above set-up. First, the laser successful results were obtained with is a Helium-Cadmium laser emitting at 441.6 nm with a TEM_{oo} mode. The coherence length of the laser is approximately 7 cm so the optical path length difference of the two interfering beams measured at the polished spot had to be less than 7 cm. Since the fiber sustained more than one mode at 441.6 nm, an exact path length within the fiber would mean solving for the path length of each mode within the fiber. This was simplified by assuming that the velocity of each mode is equal to c/n and then solving for the path length within the fiber.

Another consideration was the ratio of the beam strengths. Generally a reference to object wave ration of 3 to 1, to 6 to 1 is recommended for good holograms. In our experiments this ratio is hard to determine since the true strength of the reference or evanescent wave is unknown. A good approximation to the strength of the evanescent wave is to view the amount of light that is leaking out at the polished spot due to the index mismatch of the fiber and the gelatin. This would give information as to the lower-bound estimate of the strength of the evanescent wave. The word lower-bound is used since this would indeed be a minimum estimate due to the fact that most of the power of the evanescent wave would remain very close to the fiber and only

a small portion travels away. In the experiments performed, the ratio of the reference, or evanescent, to object beam was attempted to be kept at 3 to 1. This was achieved by not using a 50-50 beamsplitter but by using an approximately 80-20 beamsplitter and having the stronger beam enter the fiber.

4.4 SENSITIZATION OF GELATIN

In the experiments performed, sensitization of the gelatin film with ammonium dichromate [$(NH_4)_2Cr_2O_7$] also proved to be more complicated than first anticipated. The first problem encountered was the actual concentration of the ammonium dichromate. Recipes for concentration of 4% up to concentrations of 7% ammonium dichromate in water exist in the literature. Experiments performed in evanescent wave holography with conventional optical waveguides report concentrations of 1% to 2% of ammonium dichromate being used [61]. The concern for the choice of concentration in working with optical fibers is that the index of refraction of the film changes drastically from 1.54 for a concentration of 0% to 1.58 for a concentration of 3% (using a 12% gelatin solution) [61]. Since fibers with a higher core refractive index were not readily available, it was important to keep the index of refraction of the dichromated gelatin as low as possible. We thus needed to use the smallest concentration of ammonium dichromate possible. The figures just cited are for

a gelatin concentration of 12% by weight. Again since in working with optical fibers we need a very low film index, both the gelatin concentration (as discussed in section 4.2) and the ammonium dichromate concentration needed to be as low as possible but high enough to yield usable holograms.

The solution to the above problem of correct concentration has been in a way discussed in section 4.2. That is, each time a certain concentration of gelatin was selected, the test microscope slides were sensitized with concentrations of 0.5% and 1.5% of ammonium dichromate and then making simple holograms of ordinary objects was attempted. At a concentration of 0.5% of ammonium dichromate attempts of making simple holograms failed both at low and high concentrations of gelatin. At a concentration of 1.5% of ammonium dichromate, attempts of making simple holograms failed for gelatin concentrations of up to 3% but were more successful at higher concentrations.

Again a compromise had to be made between the gelatin concentration, ammonium dichromate concentration and the index mismatch tolerable between the fiber and the DCG. Best results were obtained with a gelatin concentration of 5% to 6% and an ammonium dichromate concentration of 1%.

Another practical problem was the technique of sensitization. The film needed to be sensitized after the

fiber had been aligned with the lens' and the two laser beams. This is so because if the film were sensitized before being aligned, it would have to be exposed to the laser beams for alignment and this would prematurely expose it. For this reason, the fiber was aligned and then the film was sensitized very carefully without misaligning the fiber. The film was then allowed to dry for approximately 24 hours in place and in a light tight box, again without misaligning the fiber. The actual sensitization was accomplished by dipping the fiber/slide in the ammonium dichromate for 4 to 5 minutes. The ammonium dichromate had been dissolved in deionized water.

4.5 EXPOSURE AND DEVELOPMENT

The next step in making the holograms is the exposure. Numerous attempts were made at various angles of incidence and with different exposure times. Best results were obtained with exposure times of 20 seconds and 30 seconds. The angle of incidence varied from 15 degrees to 90 degrees as shown in Figure 4.3.1.

Development of the film is fairly straightforward. To develop the film, it is first washed in running water at approximately 20 degrees Celcius for 15 minutes. As the film is pulled out of the water it is rinsed with a jet of isopropyl alcohol to remove excess water. The film is then bathed in fresh isopropyl alcohol for 2 minutes and finally

pulled out slowly while simultaneously being dried with a stream of warm air. If all steps involved in making the hologram have been successful, the hologram should now be in place.

4.6 DATA

Data is presented for three separate holograms illuminated as in Figure 2.3. The diffracted waves were measured by a detector with a wedged cap on it. The slide was carefully inserted into the wedge so only the diffracted wave being measured is incident upon the detector. Even with the precaution of using a wedged cap, a small amount of stray light was still present. The reconstructing wave was measured by a 'cut back technique' after the diffracted waves were measured. The fiber was cut near the slide without moving it with respect to the lens and the laser beam. The cut end was then cleaved and the total power in the fiber was measured. It must be realized that at the wavelength of 441.6 nm approximately 10% of the total power is in the cladding and it is this 10% which illuminates the hologram. Therefore, the efficiencies are calculated with this 10% figure and not the total power. Units are not provided for two reasons: i) the efficiency is calculated in a relative manner, ii) the detector used is a silicon detector which was not calibrated for the He-Cad wavelength of 441.6 nm.

Table 4.6.1

Incident Angle	$\bar{u}_o$ Power	η	u_o Power	η	Power in Fiber 10 %	Total
15°	.0006	3.79%	.0012	7.59%	.0158	.158
45°	.0018	4.10%	.0019	4.34%	.0438	.438
60°	.0021	2.17%	.0037	3.83%	.0965	.965

Efficiencies varied from 2.17% to 7.59%. The efficiency for u_o is generally higher than that for $\bar{u}_o$. The efficiencies are not very high and techniques for improving the efficiencies were not investigated.

Illumination in form of Figure 2.5 was not successful and a diffracted beam was not observed. Two reasons may explain the failure of this mode of illumination. First, the angular dependence of this mode of illumination is very strong. In other words, if u_o is not incident at a very definite angle, u_r is not diffracted. The second reason for this may be that upon the interaction of u_o with the hologram, a true evanescent wave is not generated along the boundary due to scattering and therefore u_r is not observed.

CHAPTER 5

5.0 CONSIDERATIONS AND DISCUSSION

In this chapter a number of topics of interest are discussed. The first topic is the mode dependence of the hologram. When light is propagating along the fiber a diffracted beam is not always seen. Only after adjusting the fiber with respect to the laser beam and changing the launching conditions, does one see a diffracted beam. Also, when the power in the fiber was monitored and maximized, the diffracted beams were not necessarily maximized. Only by changing the initial launching conditions could the diffracted beams be maximized. The reason for this may be that the hologram is most efficient to only specific propagating modes: i.e., those modes which constructed the hologram initially. Changing the launching conditions changes the mode propagation and therefore the hologram efficiency.

Mixing of two different wavelengths was also attempted. A He-Ne (633 nm) laser beam was mixed in with the He-Cad (441.6 nm) by utilizing a beamsplitter. A 100% efficient hologram would translate these different wavelengths into position. In other words the two different wavelengths would be diffracted at different angles and would thus be viewed at different positions. This phenomena was not clearly observed in our experiments. A number of reasons for this exist, the first and most important being the low efficiency holograms

obtained. Another reason is the inability to view this angular separation. Viewing the angular separation was made difficult by the large amount of the He-Ne power being leaked into the cladding and "blurring" the diffracted beams. Changing the launching conditions would result in either He-Ne being diffracted or He-Cad being diffracted. The launching conditions thus determined which wavelength was being diffracted. A very efficient hologram which separated the wavelength efficiently could be of great interest in the communications area and could be used as a type of fiber spectrometer as proposed in reference 58.

The lifetime of the hologram is also found to be rather short. Since the temperature, humidity and cleanliness of the lab environment were not controlled, the holograms deteriorated with time. One or two days after exposure (depending on the factors just mentioned), the hologram would completely deteriorate. This problem can be alleviated by encasing the hologram in a plate of glass or an optical cement. However, this was not investigated.

CHAPTER 6

6.0 CONCLUSION

The experiments performed demonstrate the feasibility of developing a grating hologram along an optical fiber. The steps involved are summarized in Table 6.1.

TABLE 6.1

Preparation of optical fiber holography

1) Blade stripping of fiber and epoxy to glass slide on 10 inch curved edge.
2) Dry overnight
3) Gelatin coating with 5 to 6 percent gelatin in de-ionized water.
4) Dry overnight in vertical position.
5) Prehardening in Kodak Rapid Fix for 15 minutes.
6) Rinse in running water for 15 minutes.
7) Dry and store.
8) Alignment of optics including fiber/slide.
9) Sensitization in 1% solution of ammonium dichromate for 4 - 5 minutes without disturbing alignment. This is done approximately 24 hours before exposure.
10) Exposure at a wavelength of 441.6 nm.
11) Development:
    a) wash in running water (T ~ 20°C) for 15 min.
    b) rinse with a jet of isopropyl alcohol for 2 min.
    c) immerse in fresh isopropyl alcohol for 2 min.
    d) Pull out slowly while simultaneously drying with a stream of warm air.

The efficiencies obtained varied from 0% to 7.5% depending on the mode of illumination. These efficiencies are fairly low but the intent of the experiment is to demonstrate only the feasibility of evanescent wave holography with optical fibers. Techniques exist to increase efficiency of the hologram and these techniques need to be further investigated. Certain modes of illumination need to be better controlled so as to improve efficiency. Temperature, humidity and cleanliness of the environment in which the experiment is performed is critical and must be controlled. Preserving the hologram by an optical cement or a plate of glass must be investigated.

The experiments performed show that evanescent wave holography with optical fibers is indeed possible and further investigations can improve upon technique and hologram efficiency.

REFERENCES

1. Albe, F., "High-speed fiber optic holography", J. Opt. 15, 6, pp. 397-402, 1984.

2. Dudderar, T. D., Gilbert, J. A., Franzel, R. A., Schamell, J. H., "Remote vibration measurement by time -averaged holographic interferometry", Proc. of the V Int. Cong. on Exp. Mech., Montreal, Canada, June 10-15, 1984, pp. 362-366, 1984. See also: Exp. Tech. 9, 1, pp. 25-27, 1985.

3. Jeong, T. H., "Update on holography with fiber optics," Proc. SPIE, Vol. 747 Practical Holography II, pp. 25-29, 1987.

4. Corke, M., Jones, J. D. C., Kersey, A. D., Jackson, D. A., "All single-mode fibre optic holographic system with active fringe stabilization," J. Phys. E., 15, 3, pp. 185-186, 1985.

5. Hadbawnik, D., "Holographische endoscopic", Optic, 45, 1, pp. 21-38, 1976.

6. Albe, F., Fagot, H., Smigielski, P., "Use of an endoscope for optical fibre holography," Proc. SPIE, Vol. 600 Progress in Holographic Applications, pp. 199 223, 1986.

7. Bjelkhagen, H. I., "Optical fibers for CW- and pulsed holography", Proc. Int. Symp. on Display Holography Vol.II, Pub. by Holography Workshops, Lake Forrest College, Lake Forest, Il 60045, pp. 73-90, 1986.

8. Bjelkhagen, H. I., Wesly, E. J., Liu, J. C., Marhic, M. E., Epstein, M., "Holographic interferometry through imaging fibers using CW and pulsed lasers", Proc. SPIE, Vol. 746 Industrial Laser Holography, pp. 201-208, 1987.

9. Rowley, D. M., "The use of a fibre-optic reference beam in a focused image holographic interferometer", Opt. and Laser Technol., 15, 4, pp. 194-198, 1983.

10. Jones, J. D. C., Corke, M., Kersey, A. D., Jackson, D. A., "Fibre optic holography", Proc. SPIE, Vol. 374 Fiber Optics, pp. 144-148, 1983.

11. Raviv, G., Marhic, M. E., Epstein, M., "Fiber optic beam delivery for endoscopic holography", Opt. Commun., 55, 4, pp. 261-266, 1985.

12. von Bally, G., "Otological investigations in living man using holographic interferometry", Holography In Medicine and

Biology, G. von Bally, ed., Springer-Verlag, pp. 198-205, 1979.

13. Jeong, T. H., "Demonstrations in holometry using fiber optics", Proc. SPIE, Vol. 746 Industrial Laser Holography, pp. 16-19, 1987.

14. Leite, A. M. P. P., "Optical fibre illuminators for holography", Opt. Commun., 28, 3, pp. 303-308, 1979.

15. Muhs, J. D., Corke, M., Prater, R. L., Sweeney, K. L., "Fiber optic holography with fringe stabilization and tunable object and reference beam intensities", Proc. SPIE, Vol. 713 Optical Fibers in Medicine, pp. 105-112, 1987.

16. Gilbert, J. A. Dudderar, T. D., Boehnlein, A. J., "Ultra low frequency holographic interferometry using fiber optics", Opt. and Lasers Eng., 5, 1, pp. 29-40, 1984.

17. Suhara, T., Nishihara, H., Koyama, J., "Far radiation field emitted from an optical fiber and its application to holography", Trans. of the IECE of Japan, Sec. E, 60, 10, pp. 533-540, 1977.

18. von Bally, G., Schmidthaus, H., Mette, W., "Gradient-index optical systems in holographic endoscopy", Appl. Opt., 23, 11, pp. 1725-1729, 1984.

19. Jones, J. D. C., Corke, M., Kersey, A. D., Jackson, D. A., "Single-mode fibre-optic holography", J. Phys. E., 17, 4, pp. 271-273, 1984.

20. Gilbert, J. A., Schultz, M. E., Boehnlein, A. J., "Remote displacement analysis using multimode fiber-optic bundles", Exp. Mech., 22, 10, pp. 398-400, 1982.

21. Uyemura, T., Ogura, Y., Yamamoto, Y., Shibata, S., "Holographic interferometry for study on hearing mechanism and contribution with fiber optics", Proc. SPIE, Vol. 192 Interferometry, pp. 209-216, 1979.

22. Bjelkhagen, H. I., "Pulsed fiber holography: a new technique for hologram interferometry", Opt. Eng., 24, 4, pp. 645-649, 1985.

23. Brunetaud, J. M., Enger, A., Berjot, M., Moschetto, Y., "The interest of optical monofibres in medical practice", Onde. Electr., 59, 2, pp. 59, 1979.

24. Bykovskii, Yu. A., Kulchin, Yu. N., Smirnov, V. L., "Use of selfoc-type optical fibers to record fourier holograms", Opt. and Spektrosk., 48, 1, pp. 155-158, 1980. See also: OSA English Trans. in Opt. Spectrosc., 48, 1, pp. 86-87, 1980.

25. von Lingelsheim, T., Ahrens, T., "A new holographic interferometer with monomode fibers for intergrated optics applications", Proc. SPIE, vol. 600 Progress in Holographic Applications, pp. 106-114, 1986.

26. Ling Sen, Zhao Jun, Xie Guo Xiang, "Study of using incoherent multitude optical fibre bundle on the image-holograph of deformation measurement," Proc. SPIE, Vol. 798 Fiber Optic Sensors II, pp. 311-315, 1987.

27. Hall, T. J., Fiddy, M. A., Ner, M. S., "Detector for an optical-fiber acoustic sensor using dynamic holographic interferometry", Opt. Lett., 5, 11, pp. 485-487, 1980.

28. Sato, R., Murata, K., "Multiplex holography using image-fiber", Appl. Opt. (USA), 25, 4, pp. 480, 1986.

29. Dudderar, T. D., Hall, P. M., Gilbert, J. A., "Holo-interferometric measurements of the thermal deformation response to power dissapation in multilayer printed wiring boards", Exp. Mechs., 25, 1, pp. 95-104, 1985.

30. von Bally, G., "Otoscopic Investigations by Holograhic Interferometry: A Fiber Endoscopic Approach Using a Pulsed Ruby Laser System", Springer Ser. Opt. Sci. (Optics in Biomedical Sciences), 31, pp. 111-114, 1981.

31. Rosen, A. N., "Holographic fundoscopy with fiber optic illumination", Opt. and Laser Technol. (GB), 7, 3, 1975.

32. Dudderar, T. D., Gilbert, J. A., Bochnlein, A. J., "Achieving stability in remote holography using flexible multimode image bundles", Appl. Opt., 22, 7, pp. 1000-1005, 1983.

33. Dudderar, T. D., Gilbert, J. A., Matthys, D. R., "Potential applications of fiber optics and image processing in industrial holo-interferometry", Proc. SPIE, vol. 746 Industrial Laser Holography, pp. 20-28, 1987.

34. Nishida, N., Sakaguchi, M., Saito, F., "Holographic coding plate: a new application of holographic memory", Appl. Opt. 12, 7, pp. 1663-1674, 1973.

35. Gilbert, J. A., Dudderar, T. D., Nose, A., "Remote displacement analysis through different media using fiber optics", Proc. of the 1983 Spring Conf. on Exp. Mech., SESA, pp. 424-430, 1983.

36. Jeong, T. H., Feferman, B. J., Bennett, C. R., "Holographic systems with HOE and optical fibers", Proc, SPIE, Vol. 615, Practical Holography, pp. 2-6, 1986.

37. Dudderar, T. D., Gilbert, J. A., "Real-time holographic interferometry through fibre optics", J. Phys. E, 18, 1, pp. 39-43, 1985.

38. Dudderar, T.D., Gilbert, J. A., "Fiber optic pulsed laser holography", Appl. Phys. Lett., 43, 8, pp. 730-732, 1983.

39. Albe, F., Fagot, H., Smigielski, P., "Use of optical fibers in pulsed holography", Proc. SPIE, Vol. 492 ECOOSA '84, pp. 324- 329, 1985.

40. Gilbert, J. A., Dudderar, T. D., Schultz, M. E., Boehnlein, A. J., "The monomode fiber - a new tool for holographic interferometry", Proc. of the 1982 Joint Conference on Exp. Mech. SESA/JSME, Oahu-Maui, Hawaii, May 23-28, pp. 920-922, 1982. See also: Exp. Mech., 22, 7, pp. 190-195, 1983.

41. Marhic, M. E., Raviv, G., Bjelkhagen, H., Epstein, M., "Coaxial fiber delivery of objective and reference beams for pulsed ruby laser holography", Tech. Digest of the OSA 1986 Topical Meeting on Holography, pp. 151-154, 1986.

42. Donskoi, E. M., Toker, G. R., "Holographic interferometer using single-mode optical fibers for measuring the properties of physical fields", Trans. in: Sov. Tech. Phys. Lett., 12, 7, pp. 334-335, 1986.

43. Gilbert, J. A., Dudderar, T. D., Nose, A., "Remote displacement analysis through different media using fiber optics", Proc. of the 1983 Spring Conf. on Exp. Mech. SESA, Cleveland, OH, May 15-19, 1983, pp. 424-430, 1983. See also: Opt. Eng., 24, 4, pp. 628-631, 1985.

44. Albe, F., Fagot, H., "The use of optical fiber in pulsed holography", Proc. SPIE, Vol. 491 High Speed Photography, pp. 771-776, 1985.

45. Barmenkov, Y., Zosimov, V., Kozhevnikov, N., Kotov, O., Lyamshev, L., Nikolaev, V., "Detection of phase-modulation signal from a fiber-optic interferometer by means of a dynamic hologram in bacteriorhodopsin", Sov. Phys. Acoust., 33, 3, pp. 334-335, 1987.

46. von Bally, G., Brune, E., Mette, W., "Holographic endoscopy with gradient-index optical imaging systems and optical fibers", Appl. Opt., 25, 19, pp. 3425-3429, 1986.

47. Gilbert, J. A., Herrick, J. W., "Holographic dilsplacement analysis with multimode-fiber optics", Exp. Mech., 21, 8, pp. 315-320, 1981.

48. Gilbert, J. A., Dudderar, T. D., Nose, A., "Remote deformation field measurement through different media using fiber optics", Opt. Eng., 24, 4, pp. 628-631, 1985.

49. Yonemura, M., Nishisaka, T., Machida, H., "Endoscopic hologram interferometry using fiber optics", Appl. Opt., 20, 9, pp. 1664-1667, 1981.

50. Robinson, D. W., "Holographic and speckle interferometry in the UK. A review of recent developments", Proc. SPIE, Vol. 814.

51. Bjelkhagen, H. I., "Fiber optics in holography", Proc. SPIE, Vol. 615 Practical Holography, pp. 13-18, 1986.

52. Jeong, T. H., Kupiec, S., "Fiber optics in holography," Proc. Int. Symp. on Display Holography Vol. II, Pub. by Holography Workshops, Lake Forrest College, Lake Forest, Il 60045, pp. 69-71, 1986.

53. Gilbert, J. A., Dudderar, T. D., "Applications of fiber optics in experimental mechanics", Proc. of the 1987 SEM Spring Conf. on Experimental Mechanics, pp. 176-183, 1987.

54. Horner, J. L., Ladman, J. E., "Holographic Optical Element (HOE) for demultiplexing in fiber optic systems", SPIE, 215, Recent Advances IN Holography.

55. Raviv, G., Marhic, M. E., Scanlon, E. F., Sener, S. F., Epstein, M., "In vivo holography of vocal cords", J. Surgical Oncology, 20, pp. 213-217, 1982.

56. Albe, F., Fagot, H., Smigielski, P., "Use of an Endoscope for Optical Fiber Holography", Progress In Holographic Applications, 600, 1985.

57. Hill, K., Fujii, Y., "Photosensitivity in optical fiber waveguides: Applications to reflection filter fabrication",Appl. Phys. Lett., 32, 10, pp. 647-649, 1978.

58. Russell, P., Ulrich, R., "Grating-fiber coupler as a high resolution spectrometer", Optics Lett., 10, 6, pp. 291-293, 1985.

59. Bennion, I., Reid, D., "High-reflectivity monomode fiber grating filters", Electronics Lett., 22, 6, pp. 343-345, 1986.

60. "Intense Beams of Ultraviolet Light", U.S. Patent No.4,725,110, Feb. 16, 1988.

61. Wuthrich, A., Lukosz, W., "Holography with Evanescent Waves", Optik, 41, 2, pp. 191-211, 1974.

62. Wuthrich, A., Lukosz, W., "Holography with Guided Waves", Applied Physics, 21, 55-64, 1980.

63. T. Suhara et al., "Waveguide holograms: A new approach to hologram integration", Optics Communications, 19, 353-358, 1976.

64. Van E. Wood et al., "Holographic formation of gratings in optical waveguiding layers", Journal of Applied Physics, 46, 1214-1215, 1975.

65. R. P. Kenan, "Theory of diffraction of guided optical waves by thick holograms", Journal of Applied Physics, 46, 4545-4551, 1975.

66. O. Bryngdahl, "Evanescent waves in optical imaging", Progress in Optics, 11, 167-221, 1973.

67. H. Nassenstein, Optik, 30, pp44, 1969.

68. P. Hariharan, "Optical Holography", Cambridge University Press, p89, 1984.

Vita

Walid Saleh was born in October 1961 in Kabul, Afghanistan. He graduated from VA TECH in 1987 with a B.S. in Physics and decided to pursue a Master's in Electrical Engineering specializing in fiber optics. His free time is spent with his wife, Jamila, and working out at the gym. A lifetime goal is to be 'lean-and-mean' and still working out at age 80.